Indian Journal of Chemical Technology
Vol. 30, September 2023, pp. 705-713
DOI: 10.56042/ijct.v30i5.5216

Thermal and mechanical properties of nanofilled poly(methyl methacrylate) nanocomposites produced by two ultrasonic methods

Abdelmoumin MEZRAI[1,2], Zoulikha Khiati[3,4] & Lahouari Mrah[1,5] *

[1]Ecole Supérieure en Génie Electrique et Energétique d'Oran, Chemin Vinical N°9, Oran, Algerié (ESGEE)

[2]Laboratoire de Chimie Organique, Substances Naturelles et Analyses (COSNA), Université Aboubakr Belkaid-Tlemcen, P.O. Box 119 Tlemcen 13000, Algeria

[3]Laboratoire de Synthèse Organique, Physico-Chimie, Biomolécules et Environement(L.S.P.B.E), Département de Génie Chimique, Faculté de Chimie, Université des Sciences et de la Technologie d'Oran Mohamed Boudiaf, USTO-MB, BP 1505, El M'naouer, Oran 31000, Algérie

[4]Département de chimie-physique, Faculté de chimie, Université des Sciences et de la Technologie d'Oran, M. Boudiaf, (USTO-MB), BP 1505 El M'naouar, 31000 Oran, Algérie

[5]Laboratory of Polymer Chemistry, Department of Chemistry, Faculty of Exact and Applied Sciences, University Oran 1 Ahmed Ben Bella, BP 1524 El M'nouer, 31000 Oran, Algeria

*E-mail: lmrah@yahoo.fr

Received 13 January 2023; accepted 14 March 2023

PPMANC1 and PMMANC2 nanocomposites have been fabricated using two reactive clays by two methods and characterized in order to estimate the impact of the different dispersion states on the mechanical properties. A simple and economical process of polymerisation is adopted to develop PMMANC nanocomposites using an Algerian clay, trying to optimize the distribution of PMMA in the clay layers. Two distinct types of organic clays have been mined, labelled as (i) benzyltrimethyl ammonium chloride (BTBA-Mag (1CEC)) and (ii) hexadecyltrimethylammonium bromide (HDTAB-MagCTA (2.5CEC)). Evaluation of the properties of the PMMANC1 and PMMANC2 nanocomposites are carried out using different physicochemical techniques. The results obtained by XRD, transmission electron microscopy reveal that the modified maghnite are well dispersed in the matrix and significant improvements in thermal properties are observed from thermal analysis. The Young module, impact resistance and tensile strength of the nanocomposites incorporating 5% organoargile are the most effective compared to the two synthesis processes.

Keywords: Poly(methyl methacrylate) (PMMA) nanocomposite, Thermomechanical, Maghnite, Dispersion

Methyl methacrylate (PMMA) is an amorphous thermoplastic compound commonly used in the manufacture of lenses and optical fibers. The properties of PMMA are many and sought after, including its excellent optical clarity, biocompatibility, high scratch resistance, weather resistance, high strength and excellent dimensional stability[1]. PMMA is also a material of technological value due to its surface resistance and light fastness of the surface [2]. To improve mechanical properties and heat resistance without compromising optical transparency, the process of fabricating PMMA/clay nanocomposites is an ideal solution[3,4]. Interfacial compatibility between nanoparticles and matrix is a criterion to ensure nanodispersion, but this alone is not enough to transform these nanoparticles from heterogeneous composition to homogeneous nanodispersion in polymer matrix. The choice of method used to disperse the organically modified filler in the host matrix is also a critical factor [5-8]. The aim of the present study is the valorization of new montmorillonite type clay as a nano-reinforcement in a polymer matrix. This is an Algerian clay from the Maghnia/Tlemecen deposit that we have chosen to disperse in poly(methyl methacrylate) (PMMA) to obtain a final material with significantly improved physical properties.

Maghnite refers to a sheet silicate of Algerian montmorillonite clay with a very high silicon and aluminium content. The advantages of using maghnite over other homogeneous catalysts are its non-toxic nature, accessibility, environmental friendliness and low purchase cost. In this study, the first part presents the synthesis by two processes as well as the comparison of two clays modified by a quaternary ammonium salt: hexadecyltrimethyl ammonium

bromide (PMMA/HDTA-Mag) and benzyl trimethyl ammonium chloride (PMMA/BTBA-Mag) aiming to improve the viscoelastic, thermal and mechanical properties of PMMA nanocomposites. The thermal and morphological properties have been studied in depth, providing a good overview of the main controllable factors that define the structure of the nanocomposite. This part of the work concerns the study of the dispersion of particles in a thermoplastic matrix in an organic medium (polymer). The second part is to study this dispersion and to establish a link between the state of dispersion and the final properties of the material, even if it is commonly accepted that a good dispersion leads to better properties, mechanical or otherwise. The present research attempts to demonstrate experimentally that the dispersion quality of the particles has a much greater influence on the mechanical properties than their size. An examination of the morphology by XRD and TEM confirmed the homogenization of the PMMANC structures and illustrated the appropriateness of the adopted dispersal technique. A comparative study of systems filled with the two synthesis processes was carried out to observe the degree of thermal stability in the first instance, and then to compare their thermal properties as a function of the two reactive clays and their unfilled equivalent. Finally, the stiffness and fracture toughness of the samples obtained by the loaded systems were evaluated in order to establish their mechanical behaviour.

Experimental Section

Materials

PMMA monomer was used in its synthetic form (Sigma-Aldrich) (Reagent Plus, ≥ 99%, Sigma Aldrich), Hexadecyltrimethyl ammonium bromide mentioned HDTABr [$N(CH_3)_3(C_{16}H_{33})$]Br (Sigma Aldrich), benzyltrimethylammonium chloride [$N(CH_3)_3(C_7H_7)$] (BTMACl; Sigma Aldrich), Benzoyl peroxide (BPO; Sigma Aldrich). All these materials were used as received from SIGMA-Aldrich, Algerian Maghnite comes from the company ENOF Maghnia (West of Algeria) and has also been processed as we received it.

The unmodified maghnite mentioned Na-Mag (Sigma Aldrich, 99%) with a cation exchange capacity =92 meq/100 g was dried at a temperature of 110°C and under vacuum for 2 days. The preparation of the modified clays (BTMA-Mag) and (HDCTA-Mag) was carried out by the cation exchange process in which the sodium ions Na^+ present in Maghnite were exchanged by benzyl tri-methyl ammonium or Cetyltrimethyl ammonium in aqueous solution following the procedure described in the literature [9-11]. This clay was organomodified with BTMACl and HDTABr, in an acidic medium, to make the clay organophilic and allow more efficient use of the clay.

In the present study, the two types of organophilic clays were compared using two in-situ polymerization processes and incorporating the PMMA polymer in solution by ultrasonication. PMMA/BTBA-Mag and PMMA/HDTA-Mag nanocomposites were prepared in two different ways. The first procedure consists of introducing a PMMA/Maghnite-Org/acetonitrile suspension into a vessel (25 mL) and benzoyl peroxide (3 wt%) as a initiator and then subjecting it to sonication using an ultrasonic bath. For the second technique, the Org-Maghnite /acetonitrile suspension was dispensed into a container (25 mL) and sonicated with a sonication needle. Once the PMMA was dissolved in acetonitrile, the polymer was added to the suspension, then the initiator benzoyl peroxide (3, wt%), under temperature control and sonicated the solution. The nominal capacity of the bath is 250 W and that of the probe is 75 W. At the end of these dispersion processes, each nanocomposite obtained at the end of the reaction was precipitated by a casting procedure in a solvent, then filtered and dried under vacuum at room temperature for 48 h. Both neat PMMA and PMMANC containing 1, 3, 5 and 7% PMMA/BTBA-Mag or PMMA/HDTA-Mag were prepared by in situ suspension polymerization [12].

Characterization

The range of Fourier transform infrared (FTIR) spectra were recoreded with an ATIMATTSON FTIR spectrometer in the 400-4000 cm^{-1} range. X-ray diffractograms of the materials were recoreded using Bruker AXS D8 Advance diffractometer with LynxEye linear detector, under Co Kα1 (λ = 1.540Å), in a 2θ scan range from 0 to 70° and at a scan speed of 0.02 °/s, at room temperature. The dispersion of nanoparticles in PMMA was examined by transmission electron microscopy (TEM) (Hitachi H800 MT at 200 kV and LEO 922 Omega at 160 kV). The checking of the degree of dispersion of the nanoparticles in PMMA and the examination of the

morphology and chemical composition of the residues were carried out with an environmental scanning electron microscope (ESEM) QUANTA FEG 200 of the company FEI. Thermogravimetric analysis (TGA) was performed with a Netzsch STA 409 PC in aluminium crucibles (150 µL) containing 15-20 mg of product to be analyzed. The mechanical properties of PMMA and nanocomposites were studied by dynamic mode mechanical analysis (Netzsch DMA 242C). Energy conservation and loss modules (E′ and E″ respectively) were measured as a function of temperature (-50°C to +160°C) with a temperature rise rate of 2 °C.min^{-1}. The measurements were carried out in the single cantilever bending mode at a frequency of cantilever mode of 1 Hz. The number and weight average molecular weights of the synthesized polymers were obtained by steric exclusion chromatography using WATERS equipment consisting of protective columns (PL gel 10 µm; 50 x 7.5 mm), two mixed-B columns (PL gel 10 µm; 300 x 7.5 mm) and a differential refractive index detector (PL-RI) [13,14] . The tensile tests were carried out at room temperature on a microcomputer-controlled universal testing machine (ZwickRoell). The initial strain rate was set at 5 mm/min.

Results and Discussion

The molecular weight and performance of PMMA

In both bath and probe polymerization processes, sterile exclusion chromatography (SEC) analysis was performed on pure PMMA and PMMA extracted from the two nanocomposites PMMANC1 and PMMANC2 of the two surfactants at the end of the polymerization. The values for weight average mass (Mw), number average mass (Mn) and intrinsic viscosity [η] are expressed in Tables 1 and 2. The PMMA masses extracted from the two nanocomposites manufactured according to the probe type ultrasonic polymerization are relatively larger than those of the bath type polymerization. This means that the propagating polymer chains (PMMA) seem to be hindered by the presence of the modified Maghnite sheets and influence the polymerization kinetics. High viscosity of the medium in the case of probe polymerization leads to a better dispersion and good distribution of the clay which would be at the origin of this behaviour. Increasing the percentage of Maghnite leads to an increase in Mn and Mw, which confirms the findings reported in the literature [15]. The presence of sufficient clay platelets in the reaction medium results in a change in the conformation of the propagating polymer chains. The interaction

Table 1 — Yield, average molecular weight (Mw), average molecular weight (Mn), polydispersity index (PDI) of PMMA and PMMAN1(PMMA/BTBA-Mag), PMMAN2(PMMA/HDTA-Mag) nanocomposite obtained by ultrasonic bath polymerization

Sample Code	Yield (wt%)	[η] (10^5) (g cm^{-3})	M_w (10^5) (g mol^{-1})	M_n (10^5) (g mol^{-1})	PDI
PMMA	71.2	0.63	1.8	0.869	2.07
PMMAN1(1wt%)	80.6	0.96	1.9	0.877	2.16
PMMAN1(3wt%)	82.1	1.35	2.15	0.923	2.32
PMMAN1(5wt%)	84.9	1.70	2.73	0.930	2.93
PMMAN1(7wt%)	71.0	1.25	2.14	0.811	2.63
PMMAN2(1wt%)	68.5	1.21	1.85	0.832	2.22
PMMAN2(3wt%)	62.4	1.39	2.12	0.865	2.45
PMMAN2(5wt%)	58.8	1.61	2.71	0.937	3.89
PMMAN2(7wt%)	49.2	1.32	1.79	0.793	2.250

Table 2 — Yield, average molecular weight (Mw), average molecular weight (Mn), polydispersity index (PDI) of PMMA and PMMAN1(PMMA/BTBA-Mag), PMMAN2(PMMA/HDTA-Mag) nanocomposite obtained by sonicated using a probe polymerization.

Sample Code	Yield (wt%)	[η] (10^5) (g cm^{-3})	M_w (10^5) (g mol^{-1})	M_n (10^5) (g mol^{-1})	PDI
PMMA	71.2	0.63	1.8	0.869	2.07
PMMAN1(1wt%)	80.6	0.96	3.32	0.867	3.26
PMMAN1(3wt%)	82.1	1.35	4.52	0.973	3.85
PMMAN1(5wt%)	84.9	1.70	4.74	0.945	4.03
PMMAN1(7wt%)	71.0	1.25	3.12	0.811	2.71
PMMAN2(1wt%)	68.5	1.21	298	0.832	2.59
PMMAN2(3wt%)	62.4	1.39	3.61	0.965	2.74
PMMAN2(5wt%)	58.8	1.61	3.74	0.777	3.81
PMMAN2(7wt%)	49.2	1.32	2.59	0.773	2.48

energy between PMMA, ammonium and clay is affected. There is a significant difference between the molar masses observed in the two procedures and for the two surfactants, which translates into a non-identical ion exchange[16]. The distribution of the polymer chains grafted in the clay does not correspond to an identical mass dispersion. A second observation was made regarding the bath process. The polydispersity index (PDI) and molar mass (Mn) values of pure PMMA and reinforced PMMA are close and therefore do not suggest a degradation of PMMA in the presence of modified maghnite (Org-Mag). We were able to observe initially and upstream of the processing, that the use of ultrasound through the probe, after a determined time and by scanning electron microscopic analysis (SEM) of the Maghnite/acetonitrile suspension, made it possible to obtain materials in which the reinforcements are well dispersed and distributed (Figures in Supplementary information). As the characteristic times of PMMA for the two samples are very close, we can state that the polymer is not degraded when the modified Maghnite is incorporated [17,18].

X-ray Diffraction Analysis

Fig. S3 shows the variety of XRD profiles obtained on Na-Mag and Org-Mag loaded Maghnite reflecting an insertion effect of the alkyl chains of the two surfactants "BTMA" and "HDTA" in the galleries of Maghnite. For a concentration level that corresponds to 1CEC, a shift of the montmorillonite peak on the (001) plane to smaller angles 2θ= 4.51° is observed; the distance between the Mag-layers increased from 12.5 Å to 18.4 Å for BTBA-Mag. However, an analysis performed on modified Maghnite (HDTA-Mag), for a concentration level corresponding to 2.5 CEC, revealed two peaks at 2θ=5.5° and 2.25° with a frequency of 19.7 Å and 39.7Å, respectively. Figs. 1(a), 1(b) shows the X-ray diffraction patterns of PMMANC1 (PMMA/BTBA-Mag(1CEC)) and PMMANC2 (PMMA/HDTA-Mag(2.5CEC)) nanocomposites, respectively, with organic fillers of 1, 3 , 5 and 7% by weight, depending on ultrasonic bath mode. Compared to BTBA-Mag (1CEC) with $d_{001} \approx 18.4$ Å, the distance between the different clay layers of the PMMANC1 (PMMA/BTBA-Mag(1CEC)) nanocomposite was nearly two-fold increased. The nanocomposites

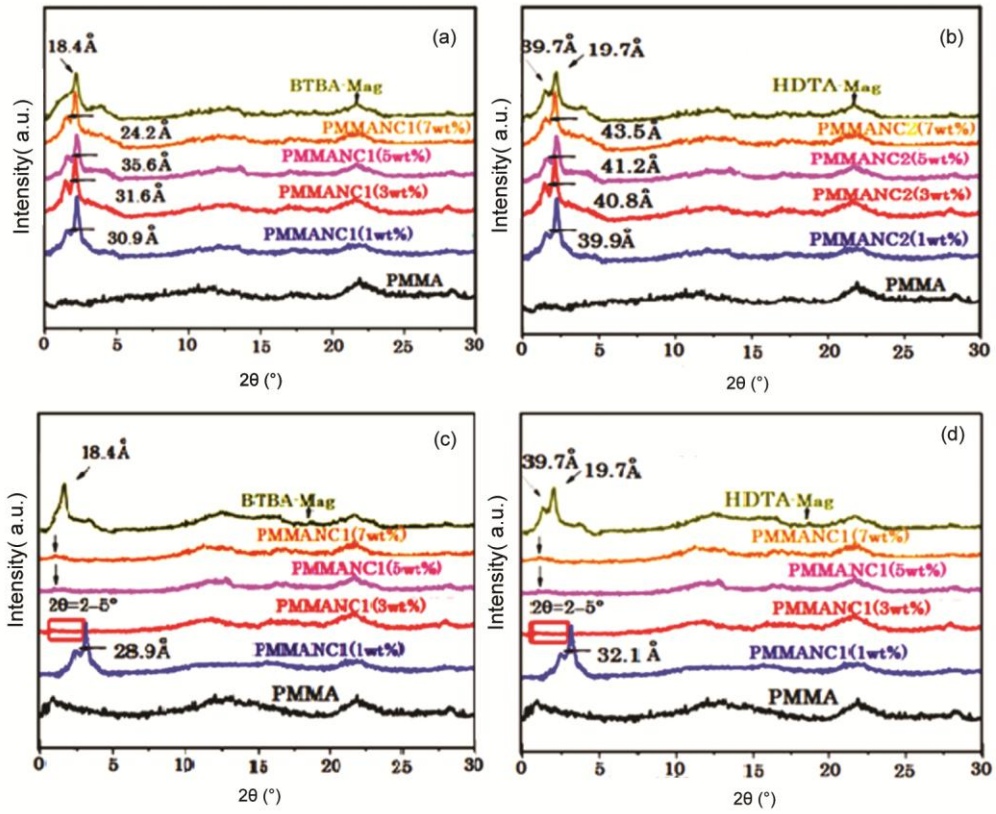

Fig. 1 — XRD patterns of (a) PMMA/ BTBA-Mag(1CEC), (b) PMMA/ HDTA-Mag(2.5CEC) nanocomposites according to the bath process and (c) PMMA/ BTBA-Mag(1CEC), (d) PMMA/ HDTA-Mag(2.5CEC) nanocomposites according to the probe process

prepared from HDTA-Mag(2.5CEC) clay also showed a small angular shift of the base d_{001} peak in the range of 2° ≈ 2.6–2.5° with interlayer distances of 39.9–43, 5 Å. The diagram in Figs. 1(c) and 1(d) illustrates the XRD profile of PMMANC1 (PMMA/BTBA-Mag(1CEC)) and PMMANC2 (PMMA/HDTA-Mag(2.5CEC)) nanocomposites, respectively, prepared at 3.5 and 7 wt% by the probe sonication process, which exhibit exfoliated morphologies, resulting in an absence of diffraction peaks at low angles. The preparation of PMMA nanocomposites containing various weight percentages (wt%) of the organomodified clay according to the bath sonication process leads to the intercalation of the polymer chains between the layers, while increasing the inter-polymer distance (Figs. 1(a), 1(b)). This type of behaviour is strongly related to a strong diffusion of PMMA in the Maghnite galleries. The process using the probe process induces a better diffusion of the PMMA matrix compared to the bath process.

Transmission Electron Microscopy Analysis

Transmission electron microscopy (TEM) analysis was performed on Na-Mag and its organically modified counterparts (BTBA-Mag(1CEC)) and (HDTA-Mag(2.5CEC)), as shown in Fig. S3. The TEM micrographs for (BTBA-Mag(1CEC)) and (HDTA-Mag(2.5CEC)), showed regularity and uniformity of interlayer spacing, indicating the existence of intercalation structure in Maghnite. Electron microscopy analysis of PMMANC1 and PMMANC2 nanocomposites containing 1, 3, 5 and 7 wt% clay confirmed the results obtained in XRD. In fact, in the presence of such modified maghnite (BTBA-Mag(1CEC)) and (PMMA/HDTA-Mag(2,5CEC)) (Figs. 2 (a) and (b)), the observed fine dispersion, is obtained by probe sonication. In contrast, no significant difference was observed between the TEM micrographs of PMMANC1 and PMMANC2 nanocomposites obtained by bath sonication. This is apparently the result of strong deconstruction of the modified maghnite after organic modification by our parent ammonium. TEM images of PMMANC1 and PMMANC2 nanocomposites obtained at high magnification by bath sonication (Figs. 2(a) and (b)). In addition, low-magnification TEM images showed some smectite-like aggregates in the nanocomposites, indicating that most of the clay platelets were well dispersed in the PMMA matrix. TEM images of nanocomposites consisting of 1, 3, 5, and 7% by weight of maghnite (Figs. 2(c) and 2(d)) visually illustrate this distribution of PMMA layers and modified maghnite. The layers of clay appeared fairly close to each other without showing any agglomerates (Figs. 2(c) and (d)). The dispersion is more even and homogeneously distributed with the PMMA/HDTA-Mag nanocomposite. The TEM images (Figs. 2(a), 2(b), 2(c) and 2(d)) clearly illustrate that the PMMA/HDTA-Mag(2.5CEC) nanocomposites compared to the nanocomposites (PMMA/BTBA-Mag(1CEC)) are significantly more compact and more uniformly distributed in the matrix. In the probe process, the shear is high and the PMMA used has smaller polymer chains, which facilitates insertion between the sheets compared to the bath process.

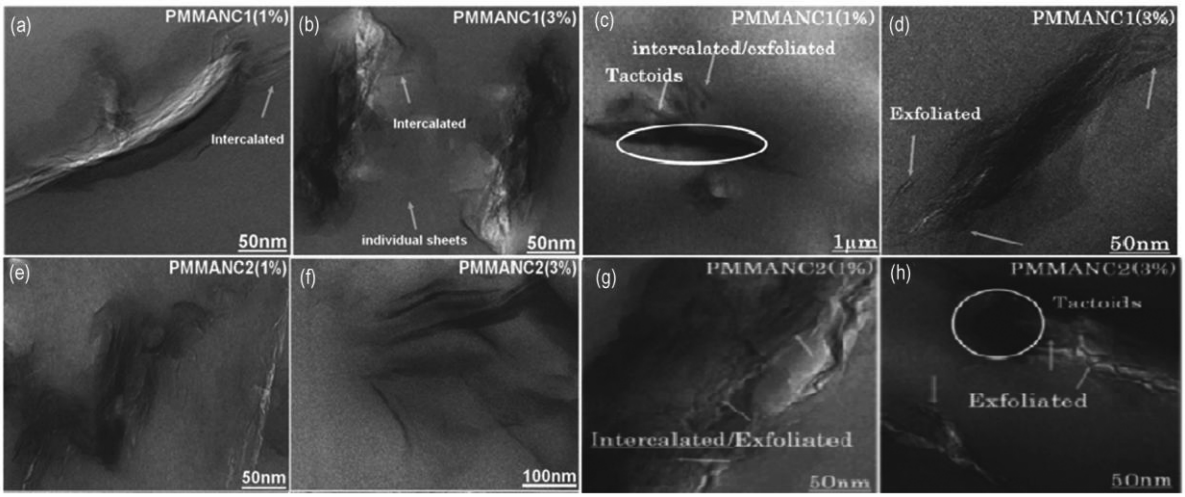

Fig. 2 — TEM images of (a) PMMA/ BTBA-Mag(1CEC), (b) PMMA/ HDTA-Mag(2.5CEC) nanocomposites according to the bath process and (c) PMMA/ BTBA-Mag(1CEC), (d) PMMA/ HDTA-Mag(2.5CEC) nanocomposites according to the probe process

Thermogravimetric Analysis

Fig. 3 shows the TG and DTG curves, where the values correspond to 20% and 50% weight loss (T20% and T50%, respectively) and the weight fraction of residues are shown. Examination of the TGA thermograms of PMMAC1 (PMMA/BTBA-Mag(1CEC)) nanocomposite showed a small improvement in thermal degradation of PMMA for nanocomposites prepared in bath sonication with different filler compositions. The T20% and T50% degradation values shown in Figs. 3(a) and 3(b) clearly show that the optimal transition to higher temperature is achieved at a rate of 5 wt%, which corresponds to 14.7°C. However, this difference remains small to assume any "nano-effect [19]. In other words, the PMMA matrix shows the same thermal behaviour in the presence and absence of this filler. A clear increase in thermodegradation temperatures is noted with this system both under air and inert atmosphere for PMMANC2 (PMMA/HDTA-Mag(2.5CEC)) nanocomposites. A shift of 35.5°C of the peak degradation maximum under air is noted for PMMA containing 5% wt in filler (Figure 3(a)). Clearly, comparison of the thermograms of the Maghnite (HDTA-Mag (2.5CEC)) prepared nanocomposites illustrates a large difference in degradation temperatures. The chain length of the surfactant (C18) by bath sonication process has a very significant impact on the thermodegradation properties. Probe sonication provides more promising results, in terms of improving the thermal properties of PMMA (Fig. 3(b)). Simple mixing of the PMMA matrix with weight percentages of organomodified Maghnite resulted in delayed degradation ($T_{50\%}$) in the range of 1.6 - 35.5°C for PMMA/BTBA-Mag(1CEC) and 20.8-44°C in the case of HDTA-Mag(2.5CEC) both in air. These figures indicate a very good improvement in the thermal properties of PMMA. The DTG curves presented in Fig.s 3(a), 3(b) illustrate the three-phase decomposition fully, with maximum degradation rates at 189, 281 and 376°C, respectively. The different degradation sequences were assigned as follows: head-to-head bond breakage in the range between 95 and 210°C, fragmentation of the polymer chain ends between 170 and 295°C and random segmentation of the PMMA chains between 290 and 450°C. The carbonized silica that remains during the heat treatment prevents oxygen in the air from propagating into the polymer and helps to reduce the rate of oxidative decomposition [20].

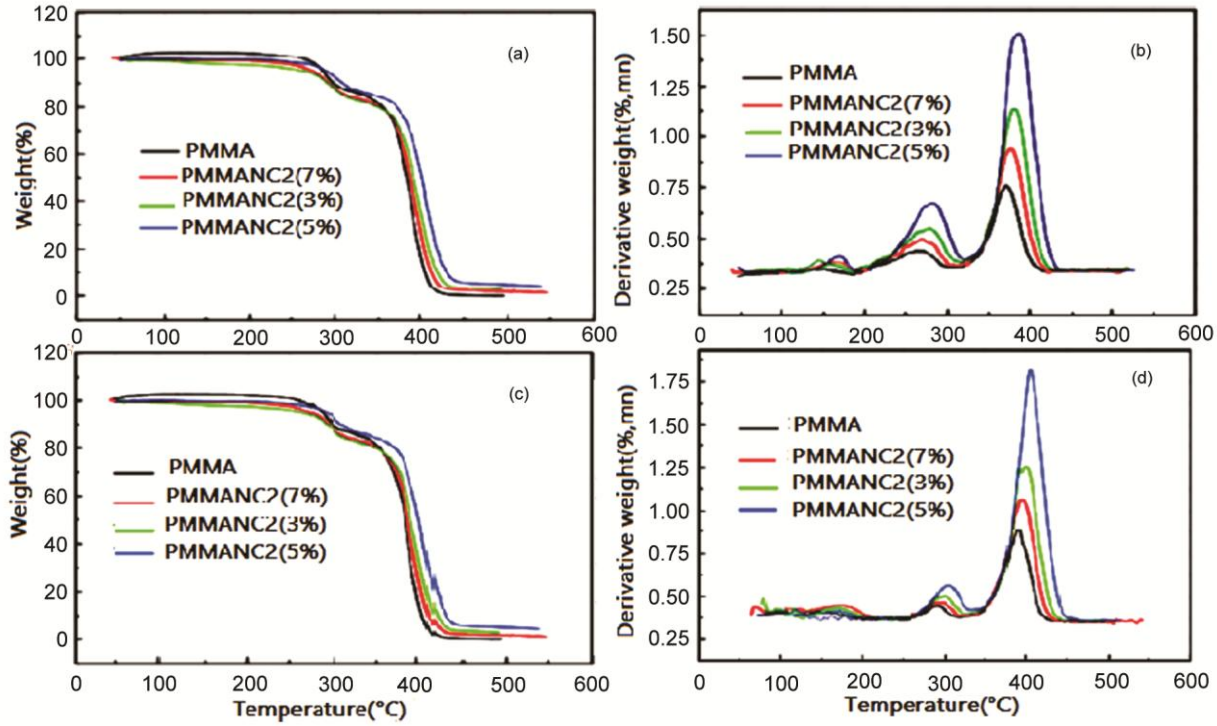

Fig. 3 — (a) TGA curves and derived thermogravimetry (DTG) data for (b) PMMA and PMMA/ HDTA-Mag(2.5CEC) nanocomposites according to the bath process and (c) TGA curves and derived thermogravimetry (DTG) data for (d) PMMA and PMMA/ HDTA-Mag (2.5CEC) nanocomposites according to the probe process

Table 3 — Mechanical data of PMMANC1 (PMMA/BTBA-Mag(1CEC)) and PMMANC2 (PMMA/HDTA-Mag(2.5CEC)) nanocomposites synthesized by probe sonication

Sample Code	Tensile strength (MPa)		Young's Modulus (GPa)		Strain at break (%)	
	Bath process	Probe process	Bath process	Probe process	Bath process	Probe process
PMMA	32.11±1.83	32.11±1.83	1.82 ±0.085	1.82 ±0.085	5.123±0.78	5.123±0.78
PMMAN1(1wt%)	32.71±1.08	34.75±1.24	1.84 ±0.097	1.86 ±0.401	2.98±0.078	3.98±1.23
PMMAN1(3wt%)	33.54±1.35	35.86±1.13	1.86 ±0.103	1.89 ±0.086	3.02±0.150	4.02±1.10
PMMAN1(5wt%)	35.71±1.03	39.13±1.81	1.88 ±0.109	1.92 ±0.095	3.58±0.078	4.58±1.78
PMMAN1(7wt%)	33.68±0.077	35.71±1.41	1.85 ±0.085	1.85 ±1.005	3.12±0.108	3.12±0.171
PMMAN2(1wt%)	35.71±0.088	36.75±1.24	1.98±0.099	2.05 ±0.223	3.65±0.123	4.65±0.232
PMMAN2(3wt%)	36.55±0.091	39.62±1.35	2.35 ±0.123	2.42 ±0.186	4.02±0.088	4.72±0.105
PMMAN2(5wt%)	39.86±1.023	44.86±2.11	2.40 ±0.109	2.83 ±0.068	4.85±0.065	4.95±0.780
PMMAN2(7wt%)	34.31±1.107	38.41±1.32	2.32 ±0.105	2.73 ±0.025	3.97±0.087	3.67±0.058

Mechanical properties

The results in Table 3 show that the maximum tensile strength of PMMANC2 (5 wt%) nanocomposites obtained by bath sonication corresponds to 39.86 MPa, which is an increase of 19.6% compared to pure PMMA, while the tensile strength of PMMANC2 (5 wt%) nanocomposites established by probe sonication reached its value of 44.86 MPa, and the percentage increased by 23.6%.In addition, the tensile strength of PMMANC2 nanocomposites obtained from HDTA-Mag(2.5CEC) clay shows improved results compared to PMMANC1 nanocomposites obtained from BTBA-Mag(1CEC) clay. According to the results obtained in Table 3, the stiffness of the nanocomposites was improved by the presence of the organic clay, and this is justified by the increase in the Young's modulus of the nanocomposites compared to that of pure PMMA. It is also found that the stiffness of our products is also proportional to the amount of filler, which is limited to a threshold of 5% by weight of the reactive clay. In contrast, the stress at break of PMMANC1 and PMMANC2 nanocomposites was reduced following mixing with the modified clay. Indeed, in the case of the bath process, stress has little tendency to modify the properties of pure PMMA, for both particle sizes. The best results in terms of improvement of Young's modulus, tensile strength and stress at break of PMMANC1 and PMMANC2 nanocomposites are observed when the organoclay nanocomposites are loaded at an optimum rate of 5 wt%, and this improvement in mechanical properties described above is satisfactory and promising when performed by the probe process compared with the bath process at different loading rates, as well as the PMMANC2 nanocomposites are better improved than the PMMANC1 counterparts. These results confirm that good dispersion leads to better mechanical properties [21].

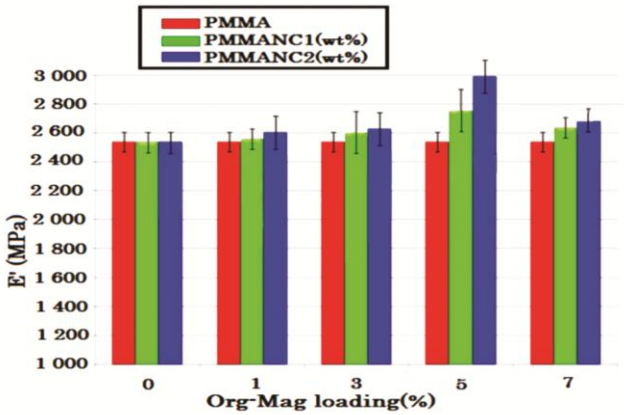

Fig. 4 — Elastic modulus (E′) of PMMA and its nanocomposites as a function of loading rate at 25°C according to the probe process

Fig. 4 shows the effect of organomodified clay on the mechanical properties (E′) obtained by dynamic mode mechanical analysis (DMA). At room temperature, PMMA exhibits a high elastic modulus (E′(25°C) = 2535 ± 67 MPa). The addition of 1-7% of the modified clay (BTBA-Mag(1CEC))and (HDTA-Mag(2.5CEC)) results in an increase in E′ (between 14 and 25% depending on the nature of the modified clay). Furthermore, this increase is observed when fillers are added to the polymer, until reaching an optimal modulus value for 5% fillers [22]. At room temperature, PMMA exhibits a high elastic modulus E′. This increase in modulus of elasticity is interesting when performed by the probe process and in the presence of Maghnite HDTA-Mag. Overall, the addition of the nanoclay has a positive effect on the Young's modulus of the material. The damping factor (tan δ) was also measured by DMA. It is the ratio of the energy loss modulus E″ and the energy

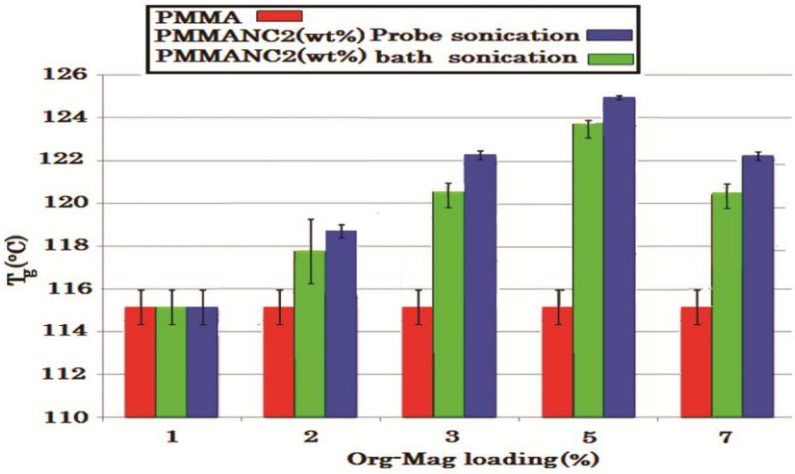

Fig. 5 — Glass transition temperature for PMMA and its nanocomposites as a function of loading ratio according to the probe process

conservation modulus E′. The values of T_g have been reported for each formulation and are presented in Fig. 5. According to Fig. 5, the T_g increases with the loading rate. For each process and active voltage, a maximum increase of 5% can be observed compared to pure PMMA (T_g PMMA = 117.8°C). The size, shape, quantity and dispersion of the particles play an important role in the mechanical behaviour of nanocomposites [23]. Indeed, a good dispersion of fillers allows interaction with a larger volume of polymer. The greater the specific surface area, the greater is the interaction.

Conclusion

The origin of the study presented in this manuscript is the mastery of the process for the dispersion of nanoparticles and the shaping of PMMANC nanocomposites from an Algerian clay. For this purpose, an ultrasound dispersion protocol was optimized using two distinct techniques and according to the presence of two different chain clays. The work carried out concerns the synthesis of poly(methyl methacrylate) nanocomposites, the physicochemical characterization of organoclays, the control of the transformation and the characterization of reinforced polymer nanocomposites. Characterization by scanning electron microscopy allowed the quantification and qualification of different dispersion states. The first process used in this study was the dispersion of organic Maghnite particles via an ultrasonic bath. It was quickly realized that this method was insufficient to disperse nano-sized particles. The protocols, developed with the ultrasound probe, allowed us to obtain dispersions of unitary Maghnite particles regardless of their size. In addition, the increase in the average molecular weight of the PMMA polymers characterized by a broad bimodal distribution was confirmed by GPC. The presence of an interphase allowed us to justify the increase in mechanical properties of the materials, an increase observed independently of the state of dispersion/distribution of the fillers and this, in spite of the low rate of incorporation of the particles.

Supplementary Information

Supplementary information is available on the website http://nopr.niscpr.res.in/handle/123456789.

References

1 Mrah L, & Khiati Z, *ChemistrySelect*, 8(29) (2023) e202301268.
2 Khiati Z & Mrah L, *Indian J Chem Technol*, 30 (2023) 173.
3 Thomas S, Thomas S & Abraham J, et al., *J Polym Res*, 25 (2018) 165.
4 Sang L, Hao W, Zhao Y, Yao L & Cui P, *e-Polym*, 18 (2018) 75.
5 Alhazime A A, El-Shamy N T, Benthami K, Barakat M M E & Nouh S A, *J Polym Eng*, 41 (2021) 119.
6 Yan S, Xue Y, Wang Z, Wang G & Wang S, *Polym Int*, 69 (2020) 933.
7 Qian X, Song L, Yu B, Shi Y, Hu Y, Richard K K & Yuen K K, *Mater Chem Phys*, 143 (2014) 1243.
8 Khiati Z & Mrah L, *Indian J Chem Technol*, 29 (2022) 117.
9 Mrah L & Meghabar R, *S N Appl Sci*, 2 (2020) 659.
10 Mrah L, Marref M & Megherbi R, *J Polym Eng*, 42 (2021) 57.
11 Khiati Z & Mrah L, *Ind J Chem Technol*, 29 (2022) 390.
12 Sardon H, Pascual A, Mecerreyes D, Taton D, Cramail H & Hedrick J L, *Macromolecule*, 48 (2015) 3153.
13 Cokoja M, Wilhelm M E, Anthofer M H, Herrmann W A & Kühn F E, *Chem Sustain Chem*, 8 (2015) 2436.
14 Khiati Z & Mrah L, *Iran Polym J*, 32(7) (2023) 829.
15 de Araújo W, Kloss J & Volpato N, *J Braz Soc Mech Sci Eng*, 43 (2021) 96.
16 Briassoulis D & Giannoulis A, *Polym Test*, 67 (2018) 99.

17 Okamoto M, Morita S, Taguchi H, Kim Y H, Kotaka T & Tateyama H, Polym, 41 (2000) 3887.
18 Janvier M, Ducrot P H & Allais F, *ACS Sustain Chem Eng*, 5 (2017) 8648.
19 Huang X & Brittain W J, *Macromolecule*, 34 (2001)3255.
20 Wang L, Xie X, Su S, Feng J & Wilkie C A, *Polym Degrad Stab*, 95 (2010) 572.
21 Yeh J M, Liou S J, Lai M C, Chang Y W, Huang C Y, Chen C P, Jaw J H, Tsai T Y & Yu Y H, *J Appl Polym Sci*, 94 (2004) 1936.
22 Moustafa H, Duquesne S, Haidar B & Vallat M F, *Polym Compos*, 38 (2017) 966.
23 Stefanovic I S, Spirkova M, Ostojic S, Stefanov P, Pavlovic V & Pergal M V, *Appl Clay Sci*, 149 (2017) 136.